GEOPHYSICAL RESEARCH LETTERS, VOL. 28, NO. 14, PAGES 2691-2694, JULY 15, 2001

Strength and elasticity of ringwoodite at upper mantle pressures

A. Kavner[1] and T. S. Duffy

Department of Geosciences, Princeton University, Princeton NJ

Abstract. The differential stress supported by a natural iron-bearing ringwoodite was determined using energy-dispersive synchrotron x-ray diffraction in a radial geometry in a diamond anvil cell. The yield strength of ringwoodite was found to increase nearly linearly from 5.8(5) GPa at a pressure of 6.2 GPa to 10.2(9) GPa at a pressure of 27.0 GPa. When scaled by the shear modulus, silicate yield strengths are systematically higher than metals, oxides, and halides at pressures up to 30 GPa. For silicates, the yield strength is 5-7% of the shear modulus in this pressure range, whereas for the other classes of solids the yield strength is typically less than 2% of the shear modulus. The results show that ringwoodite has a small postive elastic anisotropy over this pressure range.

Introduction

Understanding both the rheology and elastic properties of mantle materials is critical in modeling geodynamic behavior [*e.g. Karato & Wu, 1993*] and in interpreting tomographic images [*e.g. Grand et al., 1997*]. The Earth's transition zone is recognized as a critical region, governing chemical and thermal mixing between the Earth's upper and lower mantle through the passage of subducting slabs and rising plumes. Ringwoodite is perhaps the dominant mineral in the lower part of the transition zone [*Jackson & Rigden, 1998*], therefore its plastic and elastic behavior is of fundamental geophysical interest.

Minerals can exhibit a range of deformation behavior depending on pressure, temperature, grain size, differential stress, strain rate, and deformation history. Thus, it is of interest to examine strength and rheology across a wide range of conditions for different classes of materials [*e.g. Karato et al., 1995*]. The yield strength is a particularly significant parameter for determining the convective behavior of planetary interiors, with evidence suggesting that plate tectonics develops at low yield strengths while rigid lid behavior occurs when the yield strength is high [*Tackley, 2000*]. In the Earth's transition zone, the strengths of silicate spinels and garnets are relevant to such phenomena as slab delamination or deflection [*Karato, 1995, 1998*].

Yield strength and elasticity at high pressures are also of interest to fundamental studies of structure, bonding, and defect properties. A knowledge of material strength at high pressures is relevant to a variety of applications, including response to dynamic compression [*Steinberg et al., 1980*] and design of high-pressure devices [*Merkel et al., 1999*]. In addition, measured equations of state can be significantly in error if strength effects are not recognized and accounted for [e.g. *Kinsland, 1978; Kavner et al., 2000*]. Here we use radial diffraction techniques in the diamond anvil cell [*Singh et al., 1998a,b*] to evaluate shear strength and elastic anisotropy of ringwoodite subjected to non-hydrostatic stresses.

Experimental

Natural ringwoodite, $(Mg_{0.75}Fe_{0.25})_2SiO_4$, was extracted from the Catherwood meteorite [*Coleman, 1977*] and identified with optical microscopy, Raman spectroscopy, x-ray diffraction, and electron microprobe [*Sinogeikin et al., 1997; Kavner et al., 2000*]. The presence of minor (1-2%) impurities such as majorite garnet or plagioclase glass could not be ruled out. Two polycrystalline (~1μm crystallites) chips, each ~30x30x20 μm^3, were loaded within a ~75 μm diameter hole in a beryllium gasket, with Pt foil placed on the surface of the ringwoodite chips as a calibrant.

Radial x-ray diffraction experiments were performed at energy-dispersive beam line X17C of the National Synchrotron Light Source. The size of the incident x-ray beam was set to 20x20 μm^2 using pairs of slits. The diamond cell was positioned such that the x-ray beam passed through the sample and Be gasket, parallel to the diamond faces. Each diffraction pattern was collected at a fixed Bragg angle of $2\theta=9.044(3)^\circ$ for 15-45 minutes. At each pressure step, a series of 5 to 12 diffraction patterns were obtained by rotating the diamond anvil cell to vary the angle between the loading axis and the diffracting plane normal. Four loading steps were done in all, the first two on compression, the third on decompression, and the fourth on recompression. Details of these experiments are given elsewhere [*Singh et al., 1998a,b; Duffy et al., 1999a,b*].

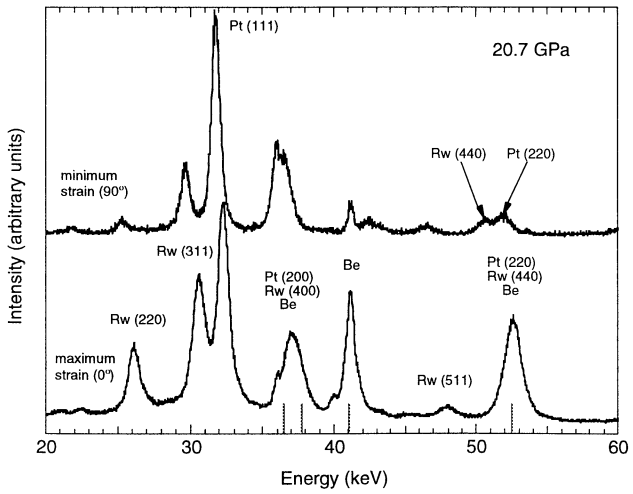

Figure 1. X-ray diffraction patterns for ringwoodite at P=20.7 GPa for the maximum and minimum strain directions. Diffraction line positions from the beryllium gasket (Be) are also shown as vertical lines.

[1]Now at Lamont-Doherty Earth Observatory, Palisades NY 10964, email: kavner@ldeo.columbia.edu

Paper number 2000GL012671.
0094-8276/01/2000GL012671$05.00

Table 1. (hkl)-Dependent Lattice Parameters of Ringwoodite.

Pressure(GPa)	Angle (deg)	*a(220)* (Å)	*a(311)* (Å)	*a(511)* (Å)
20.7(1)	0(0.5)	7.695	7.705	7.713
20.7	180	7.693	7.686	7.71
20.7	160	7.724	7.748	7.756
20.7	180	7.697	7.732	7.738
20.7	200	7.771	7.768	7.762
20.7	220	7.797	7.81	7.818
20.7	240	7.897	7.895	7.874
20.7	250	7.924	7.923	7.913
20.7	260	7.971	7.948	7.943
20.7	270	7.955	7.956	7.964
20.7	0	7.691	7.693	7.709
20.7	90	7.965	7.959	7.971
27.0(6)	0	7.641	7.647	7.644
27	90	7.924	7.905	7.918
27	70	7.88	7.87	7.874
27	110	7.874	7.874	7.875
27	180	7.629	7.612	7.634
27	165	7.638	7.64	
27	195	7.631	7.647	
27	270	7.906	7.901	7.916
27	340	7.658	7.66	7.683
27	20	7.662	7.668	7.666
27	0	7.63	7.625	
27	90	7.906	7.909	
6.2(4)	0	7.901	7.907	7.921
6.2	180	7.906	7.89	
6.2	90	8.093	8.093	8.1
6.2	20	7.892	7.914	
6.2	340	7.939	7.944	7.954
6.2	270	8.096	8.103	8.096
6.2	290	8.087	8.099	
6.2	250	8.071	8.067	
6.2	0	7.896	7.9	7.911
8.4(2)	0	7.862	7.861	7.875
8.4	180	7.859	7.851	7.874
8.4	90	8.077	8.077	8.081
8.4	20	7.88	7.885	7.88
8.4	340	7.908	7.914	7.908

[a]Pressure is determined from ringwoodite lattice parameter at 54.7°.

Samples within the diamond cell are subjected to a nonhydrostatic stress state, where the principal stress in the loading direction, σ_1, is greater than the radial stress, σ_3. The differential stress, $t=\sigma_1-\sigma_3$, experienced by a polycrystalline cubic material within a diamond anvil cell is calculated using finite strain theory assuming cylindrical symmetry and constant stress across grain boundaries (Reuss condition) through the equation [*Singh, 1993; 1998b*]:

$$\varepsilon(\psi,hkl) - \varepsilon_{hydro} = (t/3)(S_{11}-S_{12}-3S\Gamma(hkl))(1-3\cos^2\psi). \quad (1)$$

$\varepsilon(\psi,hkl)$ is the total lattice strain measured by x-ray diffraction, which varies as a function of the reflecting plane (*hkl*), and the angle between the diffracting plane normal and the maximum principal stress (ψ); ε_{hydro} is the hydrostatic component of the strain; the *Sij*'s are single crystal elastic compliances; S is a measure of the elastic anisotropy, equal to $S_{11}-S_{12}-0.5S_{44}$; and Γ is given by $(h^2k^2+k^2l^2+h^2l^2)/(h^2+k^2+l^2)^2$. According to *(1)*, at $\psi = 54.7°$, the measured lattice strain is not a function of *(hkl)*, and corresponds to the hydrostatic strain, $\varepsilon_{hydro} = (2\varepsilon_{90} + \varepsilon_0)/3$, where ε_{90} and ε_0 are the strains at the minimum and maximum stress orientations.

Results

Representative x-ray diffraction patterns are shown in Figure 1. The observed change of *d*-spacing with angle from the loading axis is dramatic: at 20.7 GPa, the ringwoodite lattice parameter shifts by 3.4% between the maximum and minimum strains, much larger than observed for any material previously studied by this technique. If the measured *d*-spacings were assumed to reflect hydrostatic strains, this would correspond to a pressure change of 34 GPa. The large observed shift in lattice parameter results in some line overlaps between ringwoodite and platinum, especially at the higher pressures. For this reason only the *(220)*, *(311)*, and *(511)* reflections were used in the analysis (Table I). In the lowest pressure run, where the *(400)* and *(440)* diffraction lines of ringwoodite are well resolved, the results using all five reflections (a_{hydro}=8.017(16) Å), and only the three above (a_{hydro}=8.009(2) Å), are within mutual uncertainties.

For an elastically isotropic material, differential stress can be determined from *(1)* and is given by [*Singh, 1993*]:

$$t = 2<\varepsilon_0-\varepsilon_{90}>G \quad (2)$$

where <> denotes the average value for all lattice reflections, and G is the shear modulus at pressure. The difference between the Voigt and Reuss bounds on the moduli in silicate spinels is negligibly small (<1%), and the corresponding difference in strength is well within the uncertainties. The minimum, maximum, and hydrostatic values of the lattice parameter were

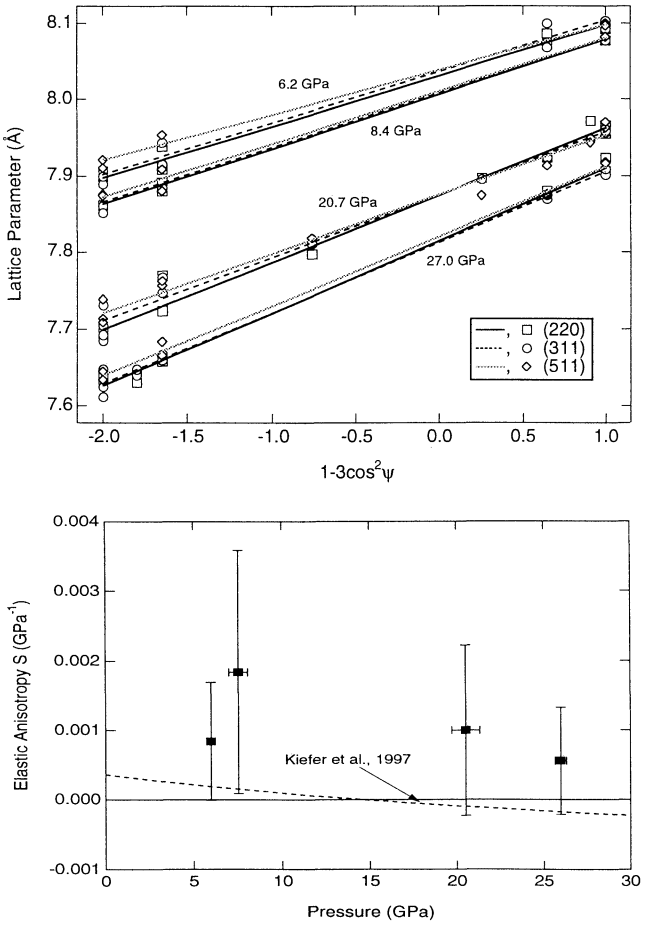

Figure 2. (a) Lattice parameter of selected ringwoodite diffraction lines versus $1-3\cos^2\psi$. (b) Elastic anisotropy, $S = S_{11}-S_{12}-0.5S_{44}$, of ringwoodite. Also shown (dashed line) are results from pseudopotential calculations of Mg end-member ringwoodite [*Kiefer et al., 1997*].

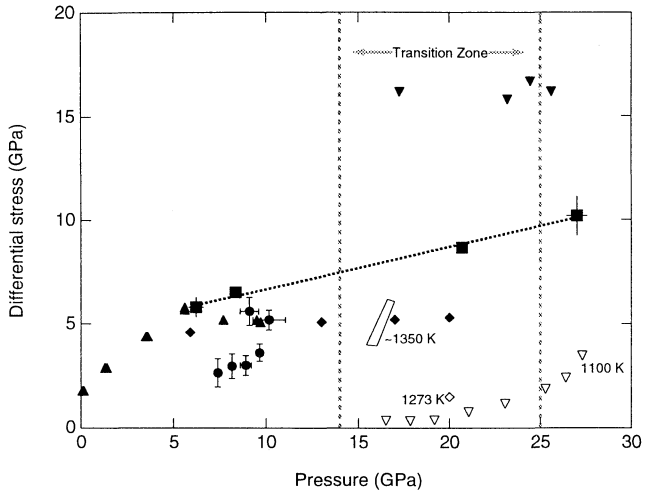

Figure 3. Measured differential stress of transition zone at room temperature (filled symbols) and high temperatures (open symbols). Lattice strain theory: ringwoodite (squares with dashed line)[*this study*], (downward pointing open triangles) [*Uchida et al, 1995*], majorite (filled circles) [*Kavner et al., 2000*]; diffraction line widths: wadsleyite (upward pointing triangles) and ringwoodite (diamonds) [*Chen et al. 1998*]; pressure gradient method: ringwoodite (downward pointing filled triangles) [*Meade and Jeanloz, 1990*]; and stress relaxation in the multi anvil press: wadsleyite (rectangular area) [*Mosenfelder et al., 2000*].

calculated by performing a linear fit of a vs. $1\text{-}3cos^2\psi$ for the *(220)*, *(311)*, and *(511)* reflections in each data set (Fig. 2a). At each pressure step, the hydrostatic Eulerian strain was calculated from the lattice parameter at ψ = 54.7° and a_0=8.118(2) Å [*Sinogeikin et al., 1997*].

Ambient-pressure Brillouin measurements on Catherwood ringwoodite supply the aggregate bulk and shear moduli, K_{0S}=193(3) GPa and G_0=113(2) GPa [*Sinogeikin et al., 1997*]. The pressure dependences of the moduli are calculated using the third-order finite strain equation assuming pressure derivatives of G' = 1.5 and K' = 4, values consistent with experimental and theoretical values for ringwoodite [*Meng et al., 1994; Kiefer et al., 1997*]. The pressure corresponding to each compression is calculated by referencing the measured hydrostatic strain to the P(V) equation of state using the Birch-Murnaghan equation.

Platinum provides an independent marker of stress in the sample chamber, and indicates a systematically lower hydrostatic pressure (by 2-4 GPa) and axial stress (by 3-5 GPa) than ringwoodite. This difference, which has been independently observed [*Hemley et al., 1997; Duffy et al., 1999a,b*], may arise from factors such as differences between strength and elastic properties of the two materials, stress gradients within the diamond cell, and sample geometry. This complication may have significant impact on equation of state studies that rely on internal markers as a pressure calibrant.

The elastic anisotropy of ringwoodite is determined from the slope of a plot of lattice parameter vs. Γ at ψ = 0° and 90° through (1) [e.g. *Duffy et al., 1999a,b*]. The results (Fig. 2b) suggest a small positive anisotropy (0.001(1) GPa^{-1}) consistent, within uncertainties, with single-crystal elasticity data for Mg end-member ringwoodite at 1 bar [*Meng et al., 1994; Jackson et al., 2000*]; and also with first-principle calculations that suggest elastic anisotropy decreases with pressure and undergoes a sign change at 17 GPa [*Kiefer et al., 1997*]. These results assume there is no plastic anisotropy. Ringwoodite's small elastic anisotropy has little effect on the strength calculation, despite assuming isotropy. This result has important implications for conventional x-ray diffraction compression studies using a near 90° geometry, where an *(hkl)*-dependent lattice parameter is often used as a diagnostic for a nonhydrostatic environment. However, the lack of an *hkl*-dependent strain does not necessarily imply hydrostaticity; even under shear, a material that is elastically isotropic (or nearly so) will show no *(hkl)*-dependence of lattice parameter.

Discussion

The measured differential stress values (Fig. 3) provide a lower bound on the yield strength of ringwoodite, based on the von Mises yielding criterion, $\sigma_y \leq (\sigma_1\text{-}\sigma_3)$, where σ_y is the yield strength. In general, transition zone silicates support significant differential stress throughout the pressure range 0-30 GPa, with a strong decrease of strength with increasing temperature (Fig. 3). However, the large variation in reported values requires further examination to identify systematic differences between techniques and to examine how material strength depends on factors such as grain size and morphology, strain rate, and total strain [*e. g. Barrett et al., 1973*].

Other measurements of the room temperature yield strength of ringwoodite show values from 5 GPa to over 16 GPa (Fig. 3). Our results are generally consistent with strength determined by examining the change in x-ray line widths with increasing stress in a multi-anvil press [*Chen et al., 1998*]. Both studies agree in the lower pressure range, showing a ringwoodite strength of ~5 GPa at ~8 GPa of pressure. The apparent flattening in Chen's data set may arise from their use of room pressure elastic moduli instead of high pressure values. On the other hand, the strengths calculated from the maximum shear

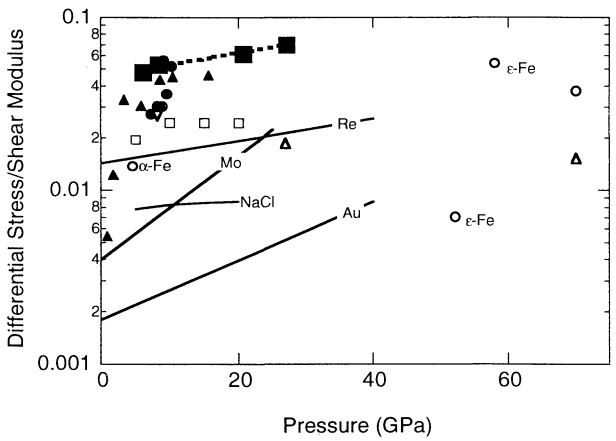

Figure 4. Summary of yield strengths determined by lattice strain techniques. Differential stress over shear modulus is plotted as a function of hydrostatic pressure (GPa) for silicates: ringwoodite (filled squares), olivine (filled triangles) [*Uchida et al., 1995*], and majorite (filled circles) [*Kavner et al., 2000*]; oxides: FeO (open downpointing triangle) [*Singh et al., 1998*]; MgO (open squares) [*Uchida et al., 1995*]; metals: Fe (open circles) [*Singh et al., 1998 and Hemley et al., 1997*]; W (open upward pointing triangles) [*Hemley et al., 1997*]; Re, Au and Mo (linear fits to data) [*Duffy et al., 1999a,b*]; and NaCl (linear fit to data) [*Funamori et al., 1994*]

stress determined by Meade and Jeanloz [*1990*] are larger by a factor of two. These authors used a technique based on measuring the pressure gradient (by ruby-fluorescence) across the diamond anvil: $\sigma_y = h\, dP/dr$, where h is the sample thickness and r is the radial distance from the center of the diamond. In addition to ringwoodite, both NaCl and MgO strengths have been studied independently using the pressure gradient technique [*Meade and Jeanloz, 1988a,b*] as well as by lattice strain theory [*Funamori et al., 1994; Duffy et al., 1995; Uchida et al., 1995*]. In all cases, lattice strain results yield a differential stress that is apparently one-half that determined by the pressure gradient method. One possibility for this discrepancy is that sample thickness may have been systematically overestimated in the pressure-gradient method.

To compare the strengths of a wide range of materials studied by lattice strain techniques, it is useful to directly examine the ratio of differential stress to shear modulus determined from the measured lattice strain (Fig. 4). Fig. 4 demonstrates that the strength of materials falls into two distinct classes: for silicates, the strength varies from ~3-7% of the shear modulus; whereas for metals, halides, and oxides the yield strength is less than 3% of the shear modulus. The ideal shear strength of a perfect crystal is estimated to be about 4-10% of the shear modulus for metals and 11-16% for oxides and halides [*Kelly and MacMillan, 1986*]. Despite enhancement of strength with pressure, the values reported in Fig. 4 still remain well below the ideal strengths. Fig. 4 also shows that the increase of strength with pressure is greater than the rise in shear modulus.

A room temperature and high pressure ringwoodite supports a higher differential stress than its low-pressure polymorph olivine. This observation is consistent among experiments exploring strength in different temperature, pressure, and/or strain rate regimes [*Karato et al., 1998; Mosenfelder et al., 2000*]. This is also consistent with high-temperature measurements on spinel and olivine polymorphs of magnesium germanates [*Dupas et al., 1998*]. These systematics suggest relationships between structure and strength that may allow us to make improved estimates about the strength of materials in planetary interiors.

Acknowledgments: We thank Dave Mao for technical assistance and helpful discussions, J. Shu, and J. Hu for experimental assistance. We also thank the Canadian Mineralogical Society and R. Jeanloz for supplying sample material. This work was supported by the NSF and the David & Lucille Packard Foundation.

References

Barrett, C. B., W. D. Nix, and A. S. Tetelman, *Principles of Engineering Materials* (Prentice-Hall, Englewood Cliffs NJ, 1973).

Chen, J., T. Inoue, D. J. Weidner, Y. Wu, and M. T. Vaughan, Strength and water weakening of mantle minerals, olivine, wadsleyite and ringwoodite, *Geophys. Res. Lett., 25*, 575-578 and 1103-1104, 1998.

Coleman, L. C., Ringwoodite and majorite in the Catherwood meteorite, *Can. Mineral., 15*, 97, 1977.

Duffy, T. S., R. J. Hemley, and H-k. Mao, Equation of state and shear strength at multimegabar pressures: Magnesium oxide to 227 GPa, *Phys. Rev. Let., 74*, 1371-1374, 1995.

Duffy, T. S., G. Shen, D. L. Heinz, J. Shu, Y. Ma, H-k. Mao, R. J. Hemley, A. K. Singh, Lattice strains in gold and rhenium under nonhydrostatic compression to 37 GPa, *Phys. Rev. B, 60*, 15063-15073, 1999a.

Duffy, T. S., G. Shen, J. Shu, H-k. Mao, and R. J. Hemley, A. K. Singh, Elasticity, shear strength, and equation of state of molybdenum and gold from x-ray diffraction under nonhydrostatic compression to 24 GPa, *J. Appl. Phys., 86*, 6729-6736, 1999b.

Dupas, C., T. N. Tingle, H. W. Green, N. Doukhan, J. Doukhan, The rheology of olivine and spinel magnesium germanate: TEM study of the defect microstructures, *Phys. Chem. Mineral., 25*, 501-514, 1998.

Funamori, N, T. Yagi, T. Uchida, Deviatoric stress measurement under uniaxial compression by powder x-ray diffraction method, *J. Appl. Phys., 75*, 4327-4331, 1994.

Grand, S. R. D. van der Hilst, and S. Widiyantoro, Global seismic tomography: a snapshot of convection in the Earth., *Geol. Soc. Amer. Today, 7*, 1-7, 1997.

Hemley, R. J., H-k. Mao, G. Shen, J. Badro, P. Gillet, M. Hanfland, and D. Hausermann, X-ray imaging of stress and strain of diamond, iron, and tungsten at megabar pressures, *Science, 276*, 1242-1245, 1997.

Jackson, I. and S. M. Rigden, Composition and temperature of the Earth's mantle: Seismological models interpreted through experimental studies of Earth materials, in *The Earth's Mantle: Composition, Structure, and Evolution*, edited by I. Jackson (Cambridge U. Press, Cambridge, 1998) pp. 405-460.

Jackson, J. M., S. V. Sinogeikin, J. D. Bass, Sound velocities and elastic properties of γ-Mg_2SiO_4 to 873 K by Brillouin spectroscopy, *Am. Mineral., 85*, 296, 2000.

Karato, S. and P. Wu, Rheology of the upper mantle: A synthesis, *Science, 260*, 771-778, 1993.

Karato, S., Z. Wang, B. Liu, and K. Fujino, Plastic deformation of garnets: Systematics and implications for the rheology of the mantle transition zone, *Earth Plan. Sci. Lett., 130*, 13, 1995.

Karato, S., C. Dupas-Bruzek, and D. C. Rubie, Plastic deformation of silicate spinel under the transition-zone conditions of the Earth's mantle, *Nature, 395*, 266-269, 1998.

Kavner, A., S. V. Sinogeikin, R. Jeanloz, J. D. Bass, Equation of state and strength of natural majorite, *J. Geophys. Res., 105*, 5963-5971, 2000.

Kelly, A., and N. H. MacMillan, *Strong Solids*, 3rd ed., (Oxford University Press, New York, 1986).

Kiefer B., L. Stixrude and R. M. Wentzcovitch, Calculated elastic constants and anisotropy of Mg_2SiO_4 spinel at high pressure, *Geophys. Res. Lett., 24*, 2841-2844, 1997.

Kinsland, G. L., The effect of strength of materials on the interpretation of data from opposed-anvil high-pressure devices, *High Temp. High Press., 10*, 627-639, 1978.

Meade, C. and R. Jeanloz, Yield strength of the B1 and B2 phases of NaCl, *J. Geophys. Res., 93*, 3270-3274, 1988.

Meade, C., and R. Jeanloz, Yield strength of MgO to 40 GPa, *J. Geophys. Res., 93*, 3261-3269, 1988b.

Meade, C., and R. Jeanloz, The strength of mantle silicates at high pressures and room temperature: implications for the viscosity of the mantle, *Nature, 348*, 533-535, 1990.

Meng, Y., Y. Fei, D. J. Weidner, G. D. Gwanmesia, and J. Hu, Hydrostatic compression of γ-Mg_2SiO_4 to mantle pressures and 700 K: thermal equation of state and related thermoelastic properties, *Phys. Chem. Minerals, 21*, 4077-412, 1994.

Merkel, S., R. J. Hemley, H-k. Mao, Finite-element modeling of diamond deformation at multimegabar pressure, *Appl. Phys. Lett., 74*, 656, 1999.

Mosenfelder, J. L., J. A. D. Connolly, D. C. Rubie, and M. Liu, Strength of $(Mg,Fe)_2SiO_4$ wadsleyite determined by relaxation of transformation stress, *Phys. Earth. Plan. Int., 120*, 63-78, 2000.

Singh, A. K., The lattice strains in a specimen (cubic system) compressed nonhydrostatically in an opposed anvil device, *J. Appl. Phys., 73*, 4278-4286, 1993.

Singh, A. K., H-k. Mao, J. Shu, R. J. Hemley, Estimation of single-crystal elastic moduli from polycrystalline x-ray diffraction at high pressure: application to FeO and iron, *Phys. Rev. Lett., 80*, 2157-2160, 1998.

Singh, A. K., C. Balasingh, H-k. Mao, R. J. Hemley and J. Shu, Analysis of lattice strains measured under nonhydrostatic pressure, *J. Appl. Phys., 83*, 7567-7575, 1998b.

Sinogeikin, S., A. Kavner, J. D. Bass, and R. Jeanloz, Elasticity of natural majorite and ringwoodite from the Catherwood meteorite, *Geophys. Res. Lett., 24*, 3265-3268, 1997.

Steinberg, D. J., S. G. Cochran, M. W. Guinan, A constitutive model for metals at high strain rate, *J. Appl. Phys., 51*, 1498-1504, 1980.

Tackley P. J., Mantle convection and plate tectonics: Toward an integrated physical & chemical theory, *Science, 288*, 2002-2007, 2000.

Uchida, T., N. Funamori, T. Ohtani, and T. Yagi, Differential stress of MgO and Mg_2SiO_4 under uniaxial stress field: variation with pressure, temperature, and phase transition, Proceedings of the 15th AIRAPT conference, Warsaw, 1996, pp. 183-185.

(Received: 11/22/00; Accepted: 05/03/01)